Influence of Preparation Conditions on Microdomain Formation in Poly(urethane urea) Block Copolymers

J. T. Garrett,† J. S. Lin,‡ and J. Runt*,†

Department of Materials Science and Engineering, The Pennsylvania State University, University Park, Pennsylvania 16802; and Oak Ridge National Laboratory, Oak Ridge, Tennessee 37831

Received May 25, 2001; Revised Manuscript Received September 10, 2001

ABSTRACT: Selected poly(urethane urea) block copolymers were prepared under different conditions and their microphase-separated morphologies analyzed primarily with small-angle X-ray scattering (SAXS). Preparation conditions were varied by adjusting the temperature and vacuum pressure during solution casting. Copolymers with relatively high hard segment contents prepared under "low" vacuum conditions, where solvent is removed comparatively slowly and the copolymers spend a longer period of time in the presence of a plasticizer (i.e., solvent), produced films with higher degrees of phase separation. The longer casting times associated with the low vacuum pressure conditions also resulted in larger mean interdomain spacings. We speculate that this may be due to secondary hard domain coalescence. Attenuated total reflectance FT-IR and wide-angle X-ray diffraction experiments were performed, but these were not sensitive to the microdomain organization of these copolymers.

I. Introduction

Polyurethane segmented block copolymers consist of amorphous, low T_g "soft" blocks chemically combined with glassy (sometimes crystalline) "hard" blocks to yield high performance materials. The degree to which the hard and soft blocks phase separate into microdomains plays a vital role in determining the solid state properties of this family of multiblock copolymers.[1−8] Phase separation in polyurethanes can be affected by a number of factors and has been investigated using a variety of techniques.

In one of our previous studies of poly(urethane urea)s [PUU] prepared from 4,4′-methylene di(*p*-phenyl isocyanate) [MDI], ethylenediamine [EDA] and 2000 g/mol poly(tetramethylene oxide) [PTMO],[9] the influence of copolymer composition on microphase separation was investigated. Despite the polarity of, and strong hydrogen bonding between, hard segments, these copolymers were found to exhibit relatively low degrees of phase separation (<45%), similar to (but somewhat higher than) those observed for other polyurethanes.[5,10,11] Mixing (or trapping) of unlike segments in the microdomains was found to be primarily responsible for the poor phase separation in the PUUs. At low hard segment contents (i.e., below 30%) phase separation values are consistent with the idea of a critical hard segment length above which hard segments phase separate.[10] As the weight fraction of hard segments increases, a greater portion of hard segments is longer than this critical length, and the degree of overall phase separation increases. This has been seen to hold true up to 70 wt % hard segments in diol-based polyurethanes.[5,12] However, the critical hard segment length model is not consistent with the experimental scattering behavior of our PUUs at hard segment contents ≥30 wt %. At these higher hard segment contents, increased hydrogen bonding presumably restricts the mobility and many hard segments apparently become trapped in the soft phase. Annealing studies (at 150 °C) were conducted in an effort to approach equilibrium, but the overall extent of phase separation was still found to be relatively low.[9] These copolymers cannot be annealed at higher temperatures due to chemical degradation, the reason that this family of multiblock copolymers must be processed from solution.

Since the influence of annealing in the absence of chemical degradation is limited, we attempted to exert control over PUU microphase morphology during solution casting. There has been some limited work on the effect of solvent casting conditions on phase separation of polyurethanes[13] and poly(urethane urea)s.[14,15] The previous studies on PUUs focused on changes in the Fourier transform infrared (FT-IR) spectra of PUU films but, although FT-IR is a valuable tool for investigating organization in PUUs,[16,17] experiments were only conducted on a single copolymer. Additionally, films used in these previous studies were relatively thin (necessarily, since transmission FT-IR experiments were conducted), and it is unclear whether the observed behavior is an accurate predictor of the properties of the material in bulk form. To more fully understand the influence of preparation conditions on the phase behavior of PUUs, six PUU multiblock copolymers were prepared under four different casting conditions and investigated using primarily small-angle X-ray scattering.

II. Experimental Section

Materials. Two series of poly(urethane urea) multiblock copolymers were synthesized via a two-step polycondensation reaction. The reactions were carried out in solution in *N*,*N*-dimethylacetamide (DMAc, 99+%, anhydrous) using a 2000 g/mol PTMO, end-capped with 4,4′-methylene di(*p*-phenyl isocyanate), and chain extended by EDA [or an EDA and 1,4-diaminocyclohexane (DACH) mixture]. The details of the synthesis are provided in a previous paper.[9] The first group consists of seven polymers with hard segment concentrations ranging from 14 to 47 wt %. Only EDA was used as the chain extender in the first set of copolymers, which is referred to in this paper as series I. All copolymers in series II have the same hard segment weight fraction (22%) but vary in the chain

* To whom correspondence should be addressed.
† The Pennsylvania State University.
‡ Oak Ridge National Laboratory.

10.1021/ma010915d CCC: $22.00
Published on Web 11/27/2001

Table 1. Details of Sample Preparation Conditions

	lo temp−lo vac	hi temp−lo vac	lo temp−full vac	hi temp−full vac
temp (°C)	50	100	50	100
vacuum (in. Hg)	10	10	∼30	∼30
evaporation rate[a] (g/cm²·min)	0.1×10^{-3}	1.3×10^{-3}	5.7×10^{-3}	25×10^{-3}

[a] The evaporation rates were determined using pure DMAc only.

extender mixture. Some EDA was replaced with DACH in order to partially disrupt packing in the hard phase. The five copolymers in series II have DACH contents ranging from 0 to 35 mol % of the diamine. The series I copolymers are identified by "PUU" followed by a number denoting the hard segment weight fraction. For the series II copolymers the hard segment weight fraction appears first, followed by the percentage of total diamine that is DACH. Six copolymers from these two series were selected for evaluation in the present study: PUU 17, PUU 22, PUU 22−35, PUU 30, PUU 37, and PUU 47.

Sample Preparation. Here, 30 mL aliquots of a 1% (by weight) polymer solution in DMAc were poured onto glass dishes measuring 50 mm in inside diameter by 25 mm in height. Solvent casting of the PUU films was done in a Napco E series vacuum oven connected to a Cartesian diver-type vacuum regulator (Ace Glass), a solvent trap, and a Fisher Scientific vacuum pump. The temperature was controlled by the oven while the vacuum pressure was controlled by the Cartesian diver. By adjusting these two parameters (temperature and pressure), we were able to control the solvent evaporation rate. Four conditions were used and, for the sake of brevity, they are referred to subsequently as "lo temp−lo vac", "lo temp−full vac", "hi temp−lo vac", and "hi temp−full vac". Each of these is described in Table 1.

Once the solvent was completely removed, the films were cut into appropriate sizes. Each film (∼100 μm thick) was cut to yield seven 1 cm² samples and one sample measuring approximately 2.5 × 1.5 cm. The larger sample was analyzed via ATR-FTIR and then subsequently cut into two 1 cm² squares. Solvent removal was assessed by monitoring the infrared bands associated with DMAc. The nine 1 cm² samples were then stacked to create a 1 cm × 1 cm × 1 mm sample suitable for SAXS experiments. As in our previous study of these copolymers,[9] all experimental 2D SAXS patterns were isotropic, indicating the absence of preferred orientation. Wide-angle X-ray diffraction (WAXD) experiments were conducted on selected samples using one of the squares from the SAXS experiments.

Small-Angle X-ray Scattering. SAXS experiments were conducted on the Oak Ridge National Laboratory 10-m pinhole collimated SAXS camera using a 20 cm × 20 cm positional sensitive proportional detector. Each polymer sample was run at two sample-to-detector distances, 1.119 and 5.119 m, to give a q range of $q = 0.0614-4.595$ nm^{-1}. Here $q = (4\pi/\lambda)\sin(\theta/2)$ where θ is the scattering angle and λ is the X-ray wavelength ($\lambda = 0.154$ nm). The two-dimensional data were azimuthally averaged to give a one-dimensional profile. Instrument background corrections and detector efficiency were determined with a ^{55}Fe radioactive sample. The relative scattering intensities were converted to absolute intensities via precalibrated secondary standards: a high density polyethylene for the low-q data and a vitreous carbon for the high-q data. The 1 and 5 m data were suitably appended to yield one data set for each sample. These data were then corrected for background noise and thermal density fluctuations. Since high-q data were available, a q-dependent background correction was performed via the method of Ruland.[18] The uncertainty in experimental data points was on the order of the size of the data symbols in the following 1D scattering profiles.

Attenuated Total Reflection—FT-IR and Wide-Angle X-ray Diffraction. Attenuated total reflection (ATR) is the infrared spectroscopy technique of choice here because the films prepared were too thick for transmission measurements. The ATR-FTIR experiments were conducted using a Biorad FTS 45 spectrometer with a horizontal flat plate ATR accessory from Pike Technologies. The ATR crystal was ZnSe with an endface angle of 45°. The substrate-facing side of the polymer film was placed against the crystal and clamped into position. Each sample was scanned 64 times at a resolution of 2 cm^{-1}, and the scans were signal averaged. All spectral absorbances fall within the range of Beer's law and have been normalized by using the aromatic region of the spectra (1400−1450 cm^{-1}, with the peak at 1412 cm^{-1} as the primary reference). The resulting sampling depth was estimated to be on the order of 1 μm.

All wide-angle X-ray diffraction experiments were performed in reflection on selected film samples on a Rigaku X-ray diffractometer operating in a theta-theta geometry using Cu Kα ($\lambda = 0.154$ nm) radiation. Samples were scanned at a rate of 1 or 2 deg/min from ca. 8−40° in 2θ, using a step size of 0.02°.

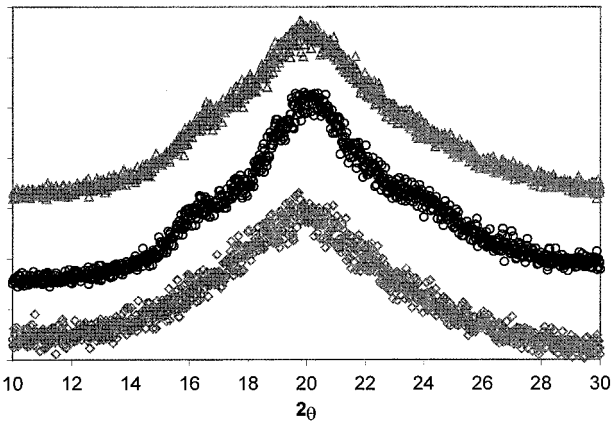

Figure 1. Representative WAXD patterns for series I copolymers: (◇) PUU 22 (hi temp−full vac); (○) PUU 37 (original conditions); (△) PUU 47 (hi temp−lo vac). The diffraction patterns are shifted vertically for the purpose of separating the curves.

III. Results and Discussion

Both wide-angle X-ray diffraction and ATR−FT-IR experiments were conducted in order to augment our SAXS study of the influence of preparation conditions on PUU domain organization. A relatively brief discussion of the results of the former experiments is presented before turning to the more enlightening SAXS results.

A. Wide-Angle X-ray Diffraction. Samples of PUU 22, PUU 30, and PUU 47 prepared using the hi temp−full vac, hi temp−lo vac, and "original" conditions were investigated using WAXD. The latter refers to the preparation method employed in our previous SAXS study[9] (i.e., dried for 24 h at ambient under "full" vacuum, followed by 24 h at 70 °C under full vacuum). None of the copolymers exhibited differences in diffraction profiles when prepared under any of the casting and drying conditions we employed.

The diffraction patterns of all of our PUU copolymers exhibit a dominant amorphous halo, with a weak shoulder appearing in the pattern of higher hard segment copolymers near $2\theta = 17°$ and, in some cases, with a very weak shoulder near 23−24°, indicating some minor level of hard segment organization. These shoulders can be seen most clearly in the diffraction pattern of PUU 37 (Figure 1). Evidence of hard segment crystallinity is commonly seen in the diffraction patterns of polyurethane copolymers having MDI−butanediol (BDO) hard segments,[19−22] and has been observed in PUUs with MDI−diethyltoluenediamine hard segments.[23,24]

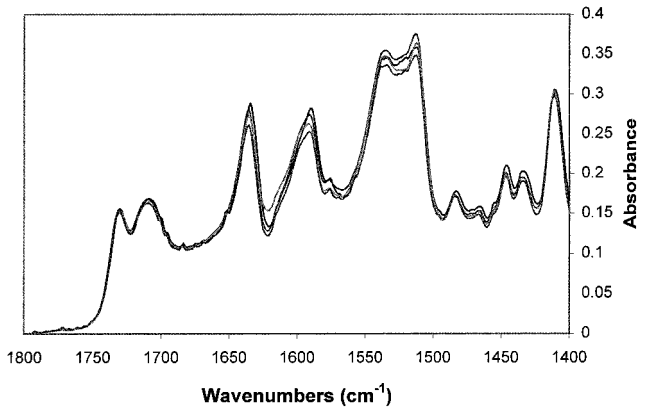

Figure 2. Influence of preparation conditions on PUU 30, ATR FT-IR spectra.

Therefore it was initially surprising, particularly for higher hard segment copolymers, that our MDI−EDA hard segments do not exhibit significant crystallinity under any of the preparation conditions explored. An explanation for this can be found by analogy to the work of Blackwell et al.[22] These authors investigated the effect of chain extender length on the crystallinity of polyurethanes, whose hard segments were prepared from MDI and diol chain extenders that varied in the number of methylene units between terminal hydroxyl groups. They found that hard segments synthesized using diols containing an even number of methylene groups (such as butanediol and hexanediol) are able to pack more efficiently in fully extended conformations and produce higher levels of crystallinity than hard segments synthesized with "odd" diols, such as pentanediol. This was found to be the case for all even diols used in their experiments except ethanediol, which was found to be too short to maximize hydrogen bonding in its extended conformation, the latter being favorable for the formation of semicrystalline hard domains. Instead, hard domains of copolymers prepared from ethanediol adopted a contracted, higher energy conformation, which leads to amorphous hard domains. It is likely that this scenario applies to our MDI−ethylenediamine based copolymers as well.

B. ATR FT-IR. ATR FT-IR spectra were acquired for samples of copolymers prepared under all conditions. As an example, the spectra for PUU 30 are shown in Figure 2. PUU 30 was chosen for display since the results of the SAXS experiments described in the next section show that these samples span the widest degree of overall phase separation of any copolymer used in our study. A spectral range from 1400 to 1800 cm^{-1} was chosen in Figure 2 to emphasize the carbonyl region as well as the aromatic region that was used to normalize the spectra. There are at least five principle peaks of interest in the carbonyl region of PUUs.[17,25] Urea carbonyls exhibit three absorbances in the urea amide I region: hydrogen bonded and ordered carbonyls (1636 cm^{-1}), hydrogen bonded and disordered carbonyls (1666 cm^{-1}) and nonbonded carbonyls (1691 cm^{-1}). In the urethane amide I region, the urethane carbonyl groups exhibit two absorbances at 1710 and 1730 cm^{-1} for the bonded and nonbonded carbonyls, respectively. The nonbonded carbonyls may not be completely "free", as the corresponding N−H in the urethane moiety may be bonded to another carbonyl or an ether oxygen of a soft segment.[17,26]

As can be seen in Figure 2, the ATR spectra of films from all four preparation conditions are essentially identical (and in all other regions of the FT-IR spectra as well) indicating no change in hard microdomain organization. The same behavior was observed for the other copolymers examined in this study. However, as noted above, microphase separation is shown in the next section by SAXS to be very significantly different for the *identical* PUU 30 samples. Clearly, ATR FT-IR is not sensitive to changes in phase behavior in the present case. This is not necessarily surprising since FT-IR probes very local organization (i.e., on the size scale of the species giving rise to the vibration, and its local environment) and does not necessarily have to correlate with microphase separation as probed by SAXS. In addition, the SAXS experiments interrogate the entire specimen while the penetration depth of our ATR FT-IR experiments was calculated to be on the order of 1 μm, only ~1% of the film thickness.

C. Small-Angle X-ray Scattering. a. Analysis of the Scattering Curves. In a previous publication, the bulk, microphase-separated morphology of the series I and II copolymers were determined using atomic force microscopy.[27] These findings led us to conclude that the most appropriate method for analyzing the SAXS profiles of these copolymers is that proposed by Bonart and Müller.[3] This approach has been covered extensively in other publications[3,8,9,11] and only the salient points will be reviewed here. For the hypothetical case of complete hard/soft segment phase separation, theoretical electron density variances ($\overline{\Delta\eta_c^2}$) can be calculated for each PUU copolymer from ideal volume fractions (ϕ) and electron densities (η)

$$\overline{\Delta\eta_c^2} = \phi_{hs}\phi_{ss}(\eta_{hs} - \eta_{ss})^2 \quad (1)$$

where the subscripts "hs" and "ss" refer to completely phase-separated hard and soft segment phases, respectively. The volume fractions are determined from bulk densities of the two phases calculated using a group contribution approach.[28] MDI units joining two PTMO segments in the absence of a chain extender ("lone" MDIs), and all PTMO units are considered as comprising the soft phase. The calculation of the concentration of lone MDIs was done following the work of Peebles[29] and is described in more detail in ref 9. The ideal hard phase is assumed to consist of the remaining MDI units and all chain extenders.

The variances calculated for the cases of complete phase separation are compared to variances derived from the experimental SAXS invariants, Q

$$Q = \int_0^\infty I(q)q^2\,dq \quad (2)$$

and experimental variances are related to the measured invariants by a constant, c. The first experimental variance is derived from the background-corrected intensity data $[I(q) - I_b(q)]$

$$\overline{\Delta\eta^{2\prime}} = c\int_0^\infty [I(q) - I_b(q)]q^2\,dq \quad (3)$$

where c is a constant $= 1.76 \times 10^{-24}$ mol^2/cm^2. The evaluation of this integral for the experimental data in the present study is straightforward since data was acquired out to sufficiently high q that the scattered intensity goes to zero at a particular q_{max}, and the same

Table 2. Interdomain Spacing and Interface Widths for PUU Copolymers Prepared under Different Conditions

	PUU 17	PUU 22−35	PUU 22	PUU 30	PUU 37	PUU 47
Interdomain Spacing (nm)						
lo temp−lo vac	15.6	12.3	15.6	13.7	15.9	14.7
hi temp−lo vac	16.2	13.3	14.2	13.1	15.3	15.0
lo temp−full vac	16.9	13.1	12.8	12.3	13.3	14.0
hi temp−full vac	15.9	12.6	12.8	12.1	13.1	14.2
Interface Width (nm)						
lo temp−lo vac	1.9	1.5	2.1	1.7	1.3	1.6
hi temp−lo vac	2.0	2.2	2.3	2.1	2.1	1.4
lo temp−full vac	2.0	1.4	2.1	1.8	1.9	2.0
hi temp−full vac	2.3	1.4	2.4	1.6	2.4	1.8

is true at low q after multiplication by q^2. A second variance based on the experimental scattering intensity can be determined by incorporating a smoothing function, $H(q)$, that models the shape of the interfacial region. Our interface profiles are assumed to be of sigmoidal shape and their characteristic value, σ, can be determined by analyzing eq 4.

$$\ln[(I(q) - I_b)q^4] = \ln K_p - \sigma^2 q^2 \tag{4}$$

In addition to σ, the Porod constant (K_p) can also be determined from eq 4. Even though the sigmoidal model is used in our calculations, the width of a linear interface model (E) is easier to visualize. The two are related by $E^2 = 12\sigma^2$ and E is listed in Table 2 along with mean interdomain spacings, ($d = 2\pi/q_{max}$, where q_{max} is the q value at the scattering peak maximum). As seen in Table 2, there is no systematic change in interfacial width with hard segment content or preparation conditions. The variance that results from "removal" of the interfaces is determined from

$$\overline{\Delta\eta^{2\prime\prime}} = c\int_0^\infty \frac{[I(q) - I_b(q)]q^2}{H(q)^2}\,dq \tag{5}$$

Insight into hard/soft segment phase separation can be obtained by comparing the variances defined in eqs 1, 3, and 5. Traditionally, overall phase separation is defined as

$$\{\overline{\Delta\eta^{2\prime}}\}/\{\overline{\Delta\eta_c^2}\} \tag{6}$$

Note that "overall phase separation" defined in this fashion is influenced by both diffuse phase boundaries and segment intermixing in the microphases. Domain boundary diffuseness can be determined by the ratio

$$(\{\overline{\Delta\eta^{2\prime\prime}}\}/\{\overline{\Delta\eta^{2\prime}}\}) - 1 \tag{7}$$

Finally, the extent of intermixing in the microdomains is obtained from

$$(\{\overline{\Delta\eta_c^2}\}/\{\overline{\Delta\eta^{2\prime\prime}}\}) - 1 \tag{8}$$

The individual variances of all samples are listed in Table 3, and the ratios defined in eqs 6−8 are presented in Table 4.

A hard or soft segment can be located in one of three environments: in a domain rich in its respective component or the interfacial region or a phase rich in the other component. If a hard segment resides in a hard domain, it contributes to the "overall phase separation". A hard segment residing in the interfacial region increases the boundary effect, and all remaining hard segments are located in the soft phase, which obviously contributes to the intermixing term. This is also the case for the soft segment. The influence of diffuse boundaries and intermixed segments are both present in $\overline{\Delta\eta^{2\prime}}$, and by comparing this value to the ideal variance calculated for the case of complete phase separation and sharp phase boundaries, we obtain a measure of the overall degree of phase separation. This is the same calculation as discussed earlier, but it is now represented in percentage form in Table 5. The variance $\overline{\Delta\eta^{2\prime\prime}}$ has had the influence of the interfaces removed, and the difference between $\overline{\Delta\eta^{2\prime}}$ and $\overline{\Delta\eta^{2\prime\prime}}$, divided by $\overline{\Delta\eta_c^2}$, provides a measure of the fraction of hard and soft segments in interfacial regions. Finally, since $\overline{\Delta\eta^{2\prime\prime}}$ is reduced from $\overline{\Delta\eta_c^2}$ only by contributions from unlike segments mixed in the microdomain, $\overline{\Delta\eta^{2\prime\prime}}-\overline{\Delta\eta_c^2}/\overline{\Delta\eta_c^2}$ represents the fraction of intermixed segments in the microphases. Note that the fractions presented are based on the total number of hard and soft segments: we cannot distinguish between mixing of hard segments in soft domains (and vice versa) using this approach.

Table 3. Electron Density Variances for PUU Copolymers

	PUU 17	PUU 22−35	PUU 22	PUU 30	PUU 37	PUU 47
		$\overline{\Delta\eta^2_c} \times 10^3$ [a]				
all conditions	2.55	4.09	4.18	6.03	7.08	8.12
		$\overline{\Delta\eta^{2\prime}} \times 10^3$				
lo temp−lo vac	0.89	1.11	1.76	1.97	2.53	2.58
hi temp−lo vac	0.90	1.01	1.68	2.39	2.57	2.47
lo temp−full vac	0.86	1.09	1.69	2.04	2.35	2.09
hi temp−full vac	0.80	1.08	1.70	1.68	2.21	2.20
		$\overline{\Delta\eta^{2\prime\prime}} \times 10^3$				
lo temp−lo vac	1.36	1.39	2.74	2.58	2.87	3.34
hi temp−lo vac	1.40	1.53	2.52	3.33	3.40	2.76
lo temp−full vac	1.34	1.29	2.63	2.66	3.06	2.75
hi temp−full vac	1.23	1.30	2.81	2.05	3.34	3.00

[a] Variances in units of (mol e/cm^3)^2.

Table 4. Electron Density Variance Ratios for PUU Copolymers

	PUU 17	PUU 22−35	PUU 22	PUU 30	PUU 37	PUU 47
		$\overline{\Delta\eta^{2\prime}}/\overline{\Delta\eta^2_c}$				
Overall Phase Separation						
lo temp−lo vac	0.35	0.27	0.42	0.33	0.36	0.32
hi temp−lo vac	0.35	0.25	0.40	0.40	0.36	0.30
lo temp−full vac	0.34	0.27	0.40	0.34	0.33	0.26
hi temp−full vac	0.31	0.26	0.41	0.28	0.31	0.27
		$(\overline{\Delta\eta^2_c}/\overline{\Delta\eta^{2\prime\prime}}) - 1$				
Diffuse Boundary						
lo temp−lo vac	0.87	1.94	0.52	1.34	1.47	1.43
hi temp−lo vac	0.82	1.68	0.66	0.81	1.08	1.94
lo temp−full vac	0.90	2.16	0.59	1.26	1.32	1.96
hi temp−full vac	1.08	2.15	0.49	1.94	1.12	1.70
		$(\overline{\Delta\eta^{2\prime\prime}}/\overline{\Delta\eta^{2\prime}}) - 1$				
Mixing in Microphases						
lo temp−lo vac	0.53	0.25	0.56	0.31	0.14	0.29
hi temp−lo vac	0.57	0.51	0.50	0.39	0.32	0.12
lo temp−full vac	0.56	0.19	0.56	0.31	0.30	0.32
hi temp−full vac	0.54	0.20	0.65	0.22	0.51	0.37

b. Influence of Preparation Conditions on Scattering Curves. The experimental, background-subtracted SAXS curves for the PUU copolymers prepared under the hi temp−lo vac condition are shown in Figure

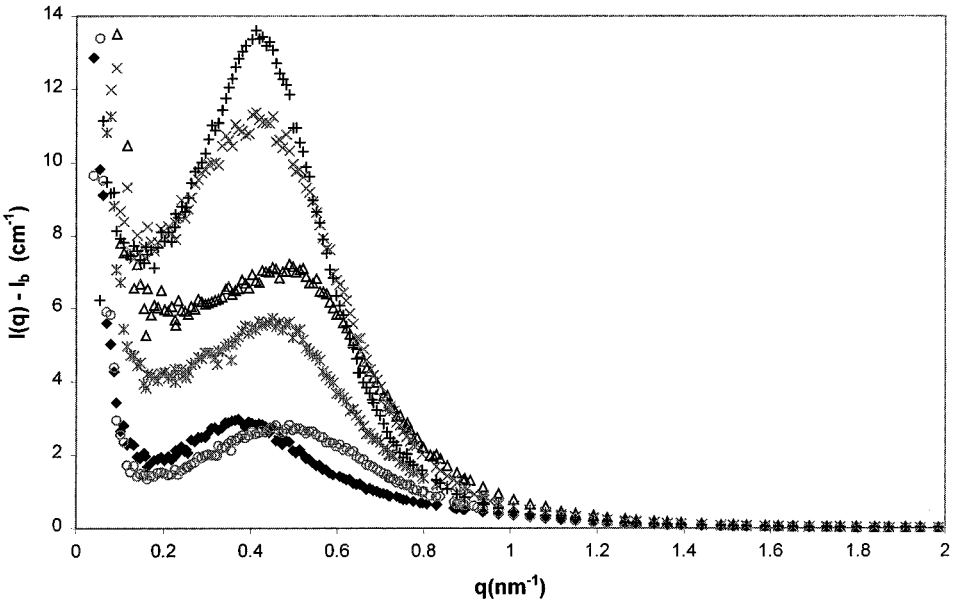

Figure 3. Background-corrected SAXS intensities as a function of scattering vector for PUU series I copolymers prepared under the hi temp−lo vac condition: (◇) PUU 17; (○) PUU 22−35; (∗) PUU 22; (△) PUU 30; (×) PUU 37; (+) PUU 47.

Table 5. Phase Separation Parameters in Percentage Form for PUU Copolymers

	PUU 17	PUU 22−35	PUU 22	PUU 30	PUU 37	PUU 47
Overall Phase Separation (%)						
lo temp−lo vac	35	27	42	33	36	32
hi temp−lo vac	35	25	40	40	36	30
lo temp-full vac	34	27	40	34	33	26
hi temp−full vac	31	26	41	28	31	27
Boundary Effect (%)						
lo temp−lo vac	19	7	24	10	5	9
hi temp−lo vac	20	13	20	15	12	4
lo temp−full vac	19	5	23	10	10	8
hi temp−full vac	17	5	27	6	16	10
Intermixing Effect (%)						
lo temp−lo vac	46	66	34	57	59	59
hi temp−lo vac	45	63	40	45	52	66
lo temp−full vac	47	68	37	56	57	66
hi temp−full vac	52	68	33	66	53	63

3. For the five copolymers with only EDA as the chain extender, the total scattering intensity increases with increasing hard segment content, primarily as a result of the change in hard domain volume fraction.[9] The experimental variances and variance ratios were determined from the scattering curves in Figure 3, as well as for the other preparation conditions (see Tables 3−5). The scatter in the data points at higher q^2 values in Porod plots (eq 4) introduce uncertainty into the calculation of the $H(q)$. The uncertainty in the slope of the fit line was determined by calculating the standard error of the slope of the regression line. This was propagated through the steps to calculate $\overline{\Delta\eta^{2\prime\prime}}$, which is used to calculate both the boundary diffuseness and degree of intermixing parameters. The estimated uncertainty in the degree of intermixing was 3%, while that of the boundary diffuseness was higher, ∼10%. (Note that these estimated errors represent the fraction of the value of the parameter they are associated with. For example, if the degree of intermixing is 25%, and the uncertainty is 3%, this means 25 ± 0.75%.) An approximate error was also determined for the parameter characterizing overall phase separation by adjusting parameters used in the analysis of the scattering curve, such as those associated with the background intensity and the appending of the 1 and 5 m data. By adjustment of these within reasonable limits, overall phase separation values were found to vary by ∼3%.

The changes in these parameters with copolymer hard segment content are similar to those reported in our previous SAXS work.[9] Overall degrees of phase separation increase with increasing hard segment content in the copolymers up to PUU 22, then decrease at higher hard segment contents. As noted earlier, the latter is likely a result of restricted hard segment mobility and the trapping of the films in a nonequilibrium condition. Note that the contribution of diffuse phase boundaries to the reduction in phase separation is relatively large for PUU 17 and PUU 22 (see Tables 4 and 5), as observed in our previous work.[9] However, measured interfacial widths are within experimental uncertainty for all copolymers, on the order of 2 nm.

For PUU 22 and PUU 22−35 (having similar $\overline{\Delta\eta_c^2}$) the scattered intensity is a direct indicator of overall phase separation. As seen in Figure 3, the experimental invariant is much smaller for PUU 22−35, indicative of a significantly lower degree of phase separation (see Table 5). The introduction of the second diamine in some PUU 22−35 hard segments disrupts inter-hard-segment hydrogen bonding and prevents the development of degrees of phase separation comparable to PUU 22.

Figure 4 illustrates the influence of preparation conditions on the scattering curves of PUU 22. Samples prepared at all four conditions have similar degrees of phase separation as calculated from eq 3 and 6 (Table 5), but the shapes of the scattering curves are somewhat different. The two samples prepared under "full vac" conditions yield scattering curves with maxima at higher q, indicative of smaller mean interdomain spacings (see Table 2). In addition, the scattering curve for the lo temp−lo vac sample exhibits additional broadening at low q (measured in terms of d) indicating asymmetric broadening of the distribution of interdomain spacings at larger sizes.

For copolymers with hard segment contents above PUU 22, the preparation conditions affect not only the

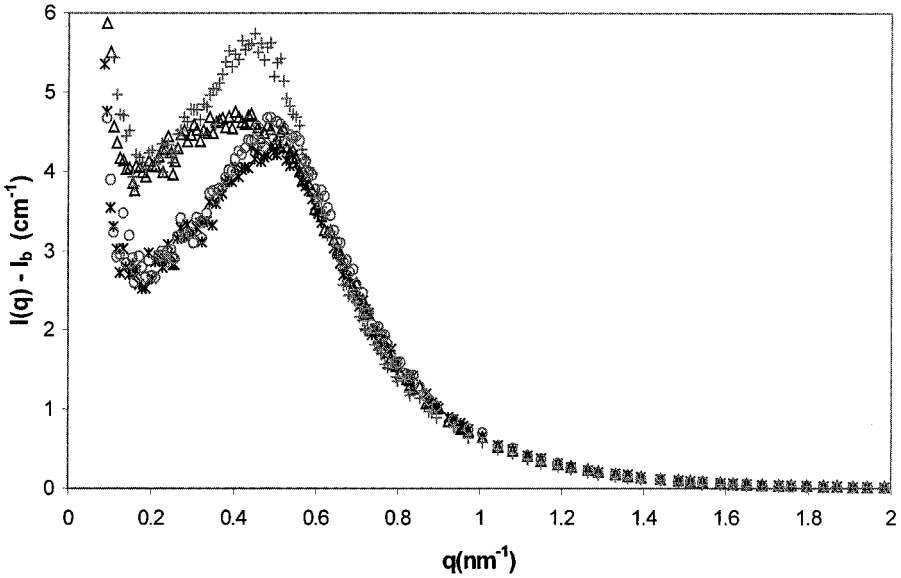

Figure 4. Background-corrected SAXS intensities as a function of scattering vector for PUU 22 prepared under various conditions: (△) lo temp−lo vac; (+) hi temp−lo vac; (∗) lo temp−full vac; (○) hi temp−full vac.

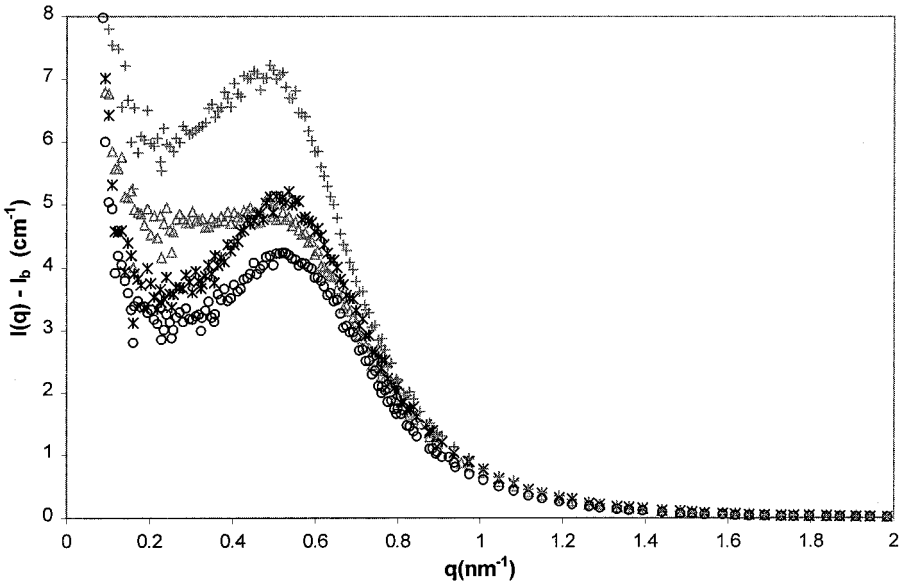

Figure 5. Background-corrected SAXS intensities as a function of scattering vector for PUU 30 prepared under various conditions: (△) lo temp−lo vac; (+) hi temp−lo vac; (∗) lo temp−full vac; (○) hi temp−full vac.

interdomain spacing but also the degree of phase separation as well. The background-corrected scattering curves for PUU 30, 37, and 47 are illustrated in Figures 5−7, respectively. The peak positions of the scattering curves of samples prepared under "full vac" conditions are observed at higher q (smaller d) than those prepared under "lo vac" conditions, similar to the behavior observed in Figure 4. In addition, there are significant differences in the degrees of phase separation depending on casting conditions. As seen in Table 5, phase separation is significantly higher for samples prepared under "lo vac" conditions, where solvent is removed relatively slowly and the copolymer spends a greater period of time in the presence of a plasticizer (i.e., DMAc).

Except for PUU 30, the degree of phase separation for the "lo vac" conditions is independent of the evaporation temperature. The behavior of PUU 30 is somewhat peculiar: the sample cast under the "hi temp−lo vac" condition has the highest degree of phase separation (40%), even though the evaporation rate of neat DMAc is approximately 10 times faster for this condition (Table 1). The origin of this difference is unknown at present but could be related to premature skinning during solvent evaporation, which could further slow solvent evaporation and permit more efficient organization. However, skinning could not be assessed since controlled evaporation took place in a vacuum oven, which prevented close inspection of the specimens as they dried. In addition, a higher temperature imparts additional mobility to the hard segments.

For copolymers containing ≥22% hard segments, interdomain spacings for samples cast under "lo vac" conditions are significantly higher than for "full vac" conditions (see Table 2). In many scattering curves of samples cast under lo vac conditions, the shift in peak position is also accompanied by peak broadening at low q. This asymmetric increase in peak breadth is most significant in lower hard segment copolymers, but is also observed in PUU 37 and 47. We speculate that both of these features arise from "secondary" hard domain

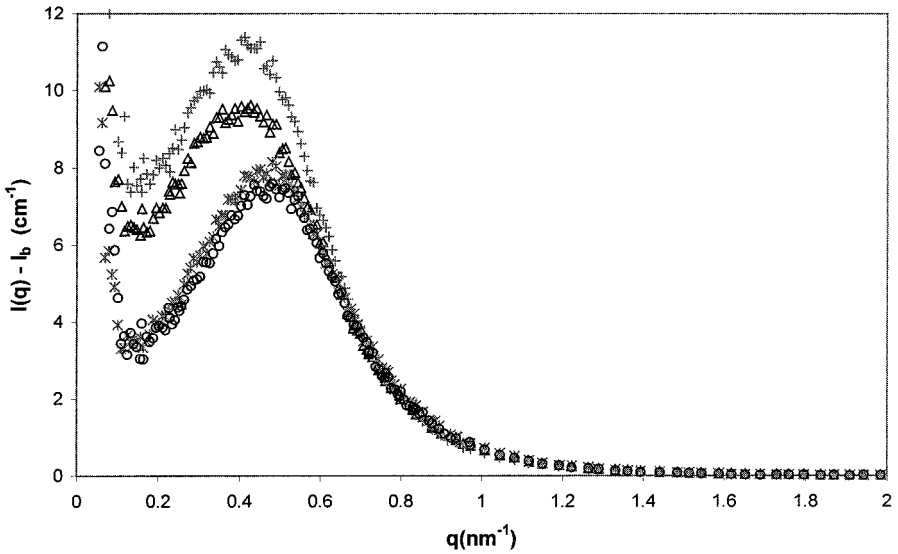

Figure 6. Background-corrected SAXS intensities as a function of scattering vector for PUU 37 prepared under various conditions: (△) lo temp−lo vac; (+) hi temp−lo vac; (∗) lo temp−full vac; (○) hi temp−full vac.

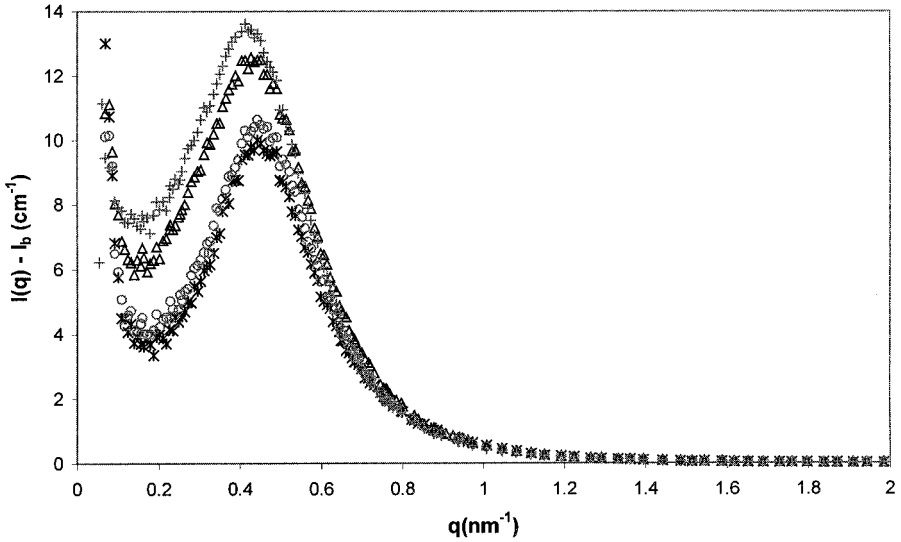

Figure 7. Background-corrected SAXS intensities as a function of scattering vector for PUU 47 prepared under various conditions: (△) lo temp−lo vac; (+) hi temp−lo vac; (∗) lo temp−full vac; (○) hi temp−full vac.

coalescence. Solvent evaporation rate is slower under "lo vac" conditions (the copolymer is plasticized by DMAc for a longer period of time) and could facilitate the coalescence of originally formed hard domains. In addition, the more pronounced low q broadening observed for the lower hard domain content copolymers likely arises from the greater mobility associated with these copolymers in which there is a smaller overall degree of hard phase hydrogen bonding hindering the mobility. The former argument follows from the work of Miller et al., who, using near-IR spectroscopy, observed a decrease in "free" PUU urethane carbonyls on annealing[30] and argued that this suggests that hard domains can approach each other and coalesce. This process would be minimized during the "full vac" conditions where the final phase-separated morphology is established relatively quickly. In addition, our results are similar to conclusions from SAXS experiments on polystyrene−polybutadiene diblock copolymers which have shown that, when quenched from the melt, microphase separation occurs rapidly, but subsequent ordering takes place on a much longer time scale.[31] Such "secondary" ordering in PUUs would lead to an increase in both the average size of hard domains as well as interdomain spacing. The latter is observed experimentally but the former is not accessible using the analysis method employed here.

IV. Conclusions

Films of selected poly(urethane urea) copolymers were solution cast at different temperatures and vacuum pressures to investigate the influence of preparation conditions on microphase separation. The films were analyzed with small-angle X-ray scattering, attenuated total reflectance FT-IR, and wide-angle X-ray diffraction. The latter two methods proved to be insensitive to changes in phase separation in this case. However, SAXS proved particularly useful in determining the influence of casting conditions. For a given preparation condition, overall degrees of microphase separation followed a trend similar to that determined in our previous study: phase separation increases with increasing PUU hard segment content up to PUU 22 and then decreases for copolymers containing higher hard

segment concentrations. The higher hard segment content copolymers presumably have restricted hard segment mobility and are trapped in a nonequilibrium condition. For individual copolymers, those prepared under low vacuum conditions exhibited a greater degree of phase separation, consistent with the longer period of time the copolymer spends in the presence of the casting solvent. In addition, lo vac conditions led to larger interdomain spacings and low q broadening of the scattering peak. We conjecture that this arises from secondary hard domain coalescence and occurs more readily for lower hard domain content copolymers due to the relatively smaller degree of hard phase hydrogen bonding hindering the mobility.

Acknowledgment. The authors would like to express their appreciation to the National Heart, Lung and Blood Institute of the NIH for partial support of this research. The research at Oak Ridge was sponsored in part by the U.S. Department of Energy under Contract No. DE-AC05-00OR22725 with the Oak Ridge National Laboratory, managed by the UT-Battelle, LLC. The authors would like to thank Dr. Michael Coleman for helpful discussions of the infrared spectroscopy data.

References and Notes

(1) Sung, C. S. P.; Hu, C. B.; Wu, C. S. *Macromolecules* **1980**, *13*, 3, 111.
(2) Sung, C. S.; Smith, T. W.; Sung, N. H. *Macromolecules* **1980**, *13*, 3, 117.
(3) Bonart, R.; Müller, E. H. *J. Macromol. Sci., Phys.* **1974**, *B10*, 177.
(4) Monteiro, E. E. C.; Fonseca, J. L. C. *J. Appl. Polym. Sci.* **1997**, *65*, 2227.
(5) Koberstein, J. T.; Leung, L. M. *Macromolecules* **1992**, *25*, 5, 6205.
(6) Christenson, C. P.; Harthcock, M. A.; Meadows, M. D.; Spell, H. L.; Howard, W. L.; Creswick, M. W.; Guerra, R. E.; Turner, R. B. *J. Polym. Sci., Polym. Phys.* **1986**, *24*, 1401.
(7) Van Bogart, J. W. C.; Gibson, P. E.; Cooper, S. L. *J. Polym. Sci., Polym. Phys.* **1983**, *21*, 65.
(8) Bonart, B.; Muller, E. H. *J. Macromol. Sci., Phys.* **1974**, *10*, 345.
(9) Garrett, J. T.; Runt, J.; Lin, J. S. *Macromolecules* **2000**, *33*, 6353.
(10) Koberstein, J. T.; Stein, R. S. *J. Polym. Sci., Polym. Phys.* **1983**, *21*, 1439.
(11) Leung, L. M.; Koberstein, J. T. *J. Polym. Sci., Polym. Phys.* **1985**, *23*, 1883.
(12) Koberstein, J. T.; Galambos, A. G.; Leung, L. M. *Macromolecules* **1992**, *25*, 6195.
(13) Brunette, C. M.; Hsu, S. L.; MacKnight, W. J. *Macromolecules* **1982**, *15*, 5, 71.
(14) Gower, L. A.; Lyman, D. J. *J. Polym. Sci., Polym. Chem.* **1995**, *33*, 2257.
(15) Ikeda, Y.; Tabuchi, M.; Sekiguchi, Y.; Miyake, Y.; Kohjiya, S. *Macromol. Chem. Phys.* **1994**, *195*, 3615.
(16) Teo, L.-S.; Chen, C.-Y.; Kuo, J.-F. *Macromolecules* **1997**, *30*, 0, 1793.
(17) Ning, L.; De-Ning, W.; Sheng-Kang, Y. *Macromolecules* **1997**, *30*, 0, 4405.
(18) Ruland, W. *Colloid Polym. Sci.* **1977**, *255*, 5, 417.
(19) Koberstein, J. T.; Galambos, A. F. *Macromolecules* **1992**, *25*, 5, 5618.
(20) Patterson, C. W.; Hanson, D.; Redondo, A.; Scott, S. L.; Henson, N. *J. Polym. Sci., Polym. Phys.* **1999**, *37*, 2303.
(21) Schneider, N. S.; Desper, C. R.; Illinger, J. L.; King, A. O.; Barr, D. *J. Macromol. Sci., Phys.* **1975**, *11*, 527.
(22) Blackwell, J.; Nagarajan, M. R.; Hoitink, T. B. *Polymer* **1982**, *23*, 950.
(23) Yuying, X.; Zhiping, Z.; Dening, W.; Shengkang, Y.; Junxian, L. *Polymer* **1992**, *33*, 1335.
(24) Ning, L.; De-Ning, W.; Sheng-Kang, Y. *Polymer* **1996**, *37*, 3577.
(25) Ning, L.; De-Ning, W.; Sheng-Kang, Y. *Polymer* **1996**, *37*, 3045.
(26) Coleman, M. M.; Skrovanek, D. J.; Hu, J.; Painter, P. C. *Macromolecules* **1988**, *21*, 59.
(27) Garrett, J. T.; Siedlecki, C. A.; Runt, J. *Macromolecules* **2001**, *34*, 7066.
(28) Coleman, M. M.; Graf, J.; Painter, P. *Specific Interactions and the Miscibility of Polymer Blends*; Technomic Publishing: Lancaster, PA, 1991.
(29) Peebles, L. H., Jr. *Macromolecules* **1976**, *9*, 58.
(30) Miller, C. E.; Edelman, P. G.; Ratner, B. D.; Eichinger, B. E. *Appl. Spectrosc.* **1990**, *44*, 581.
(31) Harkless, C. R.; Singh, M. A.; Nagler, S. E.; Stephenson, G. B.; Jordan-Sweet, J. L. *Phys. Rev. Lett.* **1990**, *64*, 2285.

MA010915D